

HETEROCYCLES, Vol. 104, No. 11, 2022, pp. 1954 - 1965. © 2022 The Japan Institute of Heterocyclic Chemistry
Received, 30th July, 2022, Accepted, 26th August, 2022, Published online, 6th September, 2022
DOI: 10.3987/COM-22-14731

REACTION PATHWAY AND KINETIC STUDY OF 4,5-DIHYDROXYIMIDAZOLIDINE-2-THIONE SYNTHESIS BY HPLC AND NMR

Liudmila Kalichkina,* Dmitry Novikov, Oleg Kotelnikov, Viktor Malkov, and Alexey Knyazev

Laboratory of Organic Synthesis, National Research Tomsk State University, 49, Arkadia Ivanova st., 634028 Tomsk, Russia; E-mail: kalichkina_lyuda@mail.ru.

Abstract – Process of 4,5-dihydroxyimidazolidine-2-thione (DHIT) synthesis from thiourea and glyoxal is studied. Formation of 1,3-dihydro-2*H*-imidazole-2-thione and 4,5-dihydroxyimidazolidin-2-one as byproducts is confirmed by NMR. The kinetics of the scalable DHIT synthesis process is studied by HPLC, and the kinetic parameters of the model based on the proposed reaction scheme are calculated. The model correctly describes the kinetics of the DHIT formation and thiourea consumption.

INTRODUCTION

4,5-Dihydroxyimidazolidine-2-thione (DHIT) is a heterocyclic compound formed by the interaction of thiourea with glyoxal (Figure 1).¹

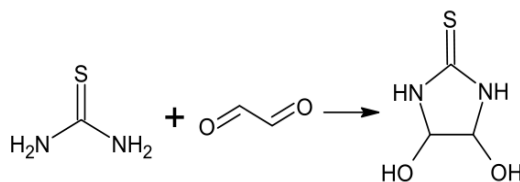


Figure 1. DHIT synthesis reaction

The DHIT is a molecular building block to produce macrocyclic semithioglycolurils and semithiobambusurils,² strongly binds anions inside the macromolecule, and the presence of sulfur in the structure allows binding metal ions at their sulfur-edged portals that distinguishes them from the oxygen-containing bambusurils.^{3,4} These properties allow them to be used to treat the channelopathies, in

supramolecular chemistry, anion sensing and catalysis.⁵ Imidazolidine-2-thiones were shown to act as ligands for transition metals.⁶ In addition, the DHIT is an effective inhibitor of acid corrosion.⁷

Thiourea interaction with glyoxal in the presence of water-soluble alcohol mainly produces a mixture of *cis*- and *trans*-DHIT isomers and urea and 2-thioimidazole are formed as byproducts.^{1,8} As known, a bicyclic product, 1,4-diaza-3,6-dithiabicyclo[3.3.0]octane-2,5-diimine, is formed in strongly acidic conditions.⁹ However, no experimental confirmation of the formation of byproducts has been presented, and the pathway for the origin of the impurities is unclear. The kinetics of the thiourea interaction with glyoxal has not been investigated, unlike substituted thiourea with substituted dialdehydes.¹⁰ In the references,^{11,12} a pathway for aldehyde reaction with nitrogen-containing organic compounds was studied by DFT and NMR. In the reference,¹³ the conditions of HPLC analysis of DHIT were developed.

In the reference,⁷ a scalable method of producing DHIT was proposed, but a thorough understanding of the reactions taking place in the system is necessary for its successful transfer to the industrial level.

The purpose of this work is to identify the byproducts forming during the DHIT synthesis, to study the pathways of its formation as well as the process kinetics for a scalable synthesis process required to manage the process when moving to an industrial scale.

RESULTS AND DISCUSSION

Study of DHIT synthesis kinetic by HPLC

An assay procedure to determine DHIT and thiourea concentrations was developed by the authors.¹³ Figure 2 shows a typical chromatogram of the *cis*- and *trans*-DHIT mixture.

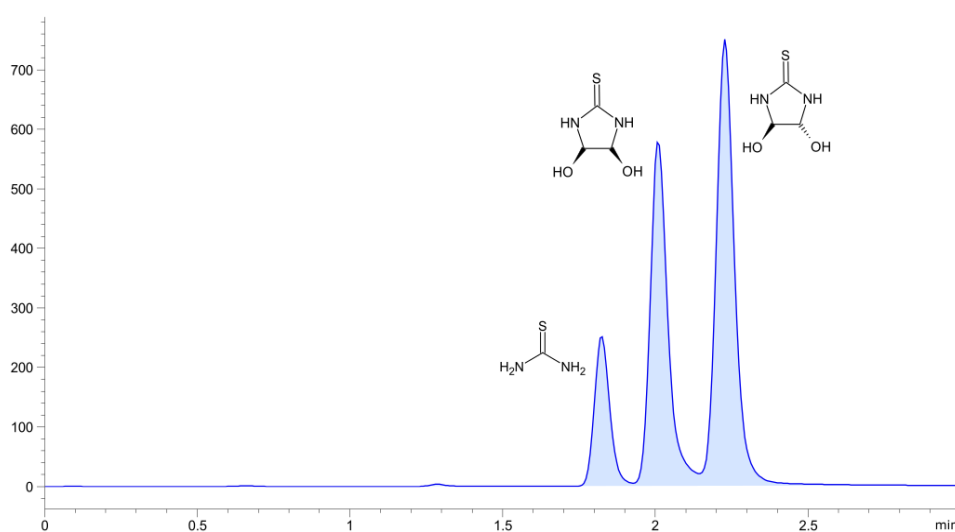


Figure 2. Chromatogram of the reaction mixture on Luna HILIC 200 Å 4.6×150 mm, 5 µm particle size (Phenomenex, USA); mobile phase was MeCN:Water 97v/3v

Thiourea had a minimal retention factor (0.42) since its retention depended on the polarity of the molecule. The retention factors for *cis*- and *trans*-DHIT were 0.58 and 0.73, respectively, because the separation of geometrical isomers depended on the steric location of hydroxyl groups. Thereby, concentration curves for DHIT and thiourea in time were obtained as a result of the kinetic experiment (Figure 9). The thiourea change ratio was 98.8% but the DHIT yield was ~65%. These results indicated the concurrent reactions in the process. The NMR spectroscopy methods were used to determine the concurrent reaction products.

Investigation of reaction products by NMR spectroscopy

Figure 3 shows the ^1H NMR spectrum of the concentrated reaction mixture in $\text{DMSO-}d_6$. There are signals related to DHIT, signals at 8.86 ppm and 8.67 ppm can be assigned to protons in amino-groups in *trans*-, *cis*-DHIT; at 5.03 ppm and 4.73 ppm protons of the methine groups in *trans*-, *cis*-DHIT, respectively.

^1H NMR spectrum of the reaction mixture in $\text{H}_2\text{O}/\text{D}_2\text{O}$ and the same mixture in $\text{DMSO-}d_6$ showed similar results. The ^1H NMR spectrum in $\text{H}_2\text{O}/\text{D}_2\text{O}$ featured a wide signal of water at 5 ppm, and the absence of the signal splitting into doublets.

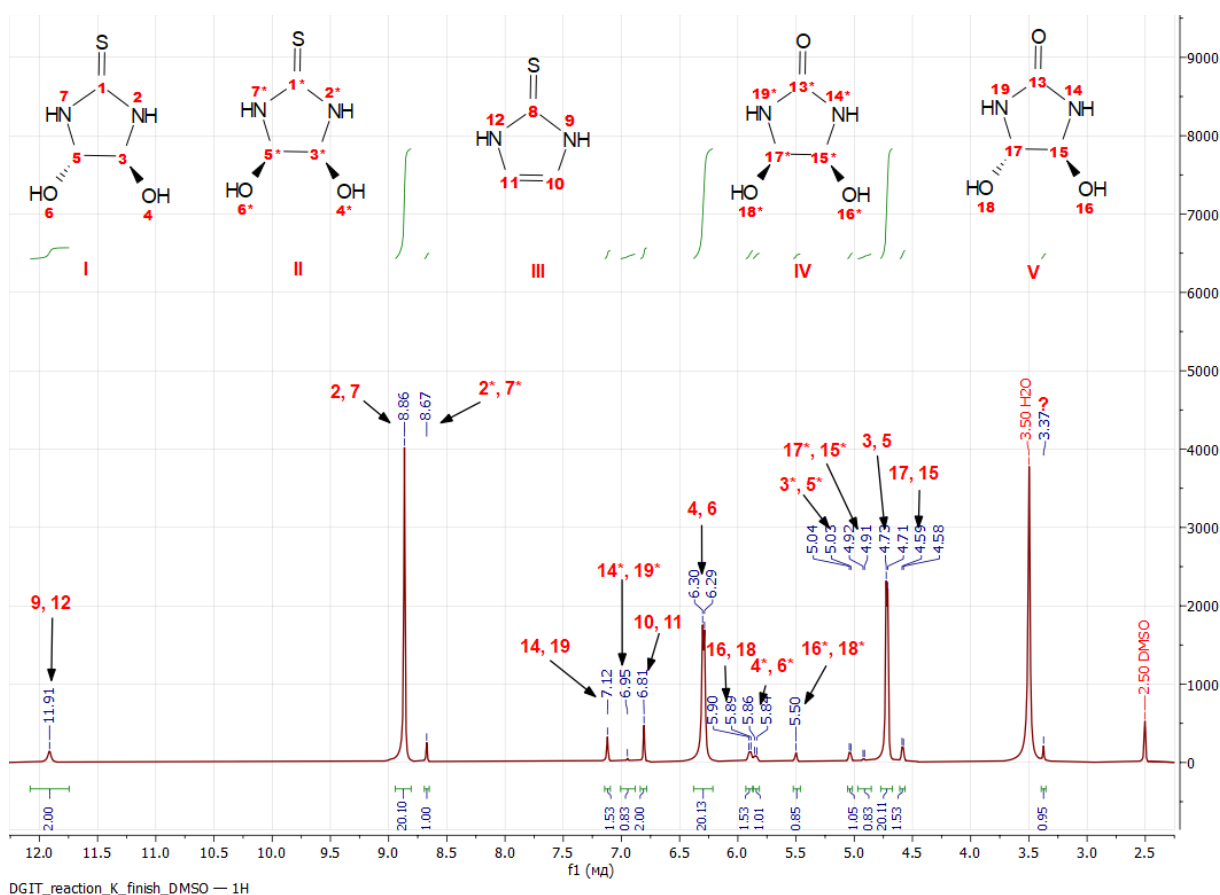


Figure 3. ^1H NMR spectrum of concentrated reaction mixture in $\text{DMSO-}d_6$

The signals at 182.11 and 181.35 ppm can be assigned to thioamide groups of *trans*-, *cis*-DHIT, while those at 87.22 and 79.95 ppm can be assigned to the methine groups of *trans*-, *cis*-DHIT in the ^{13}C NMR spectrum (Figure 4).¹³ However, the signals appeared as "doublets", and the difference between the chemical shifts of the neighboring signals were 0.06-0.14 ppm in the ^{13}C NMR spectrum of the reaction mixture in $\text{H}_2\text{O}/\text{D}_2\text{O}$ (Table 1).

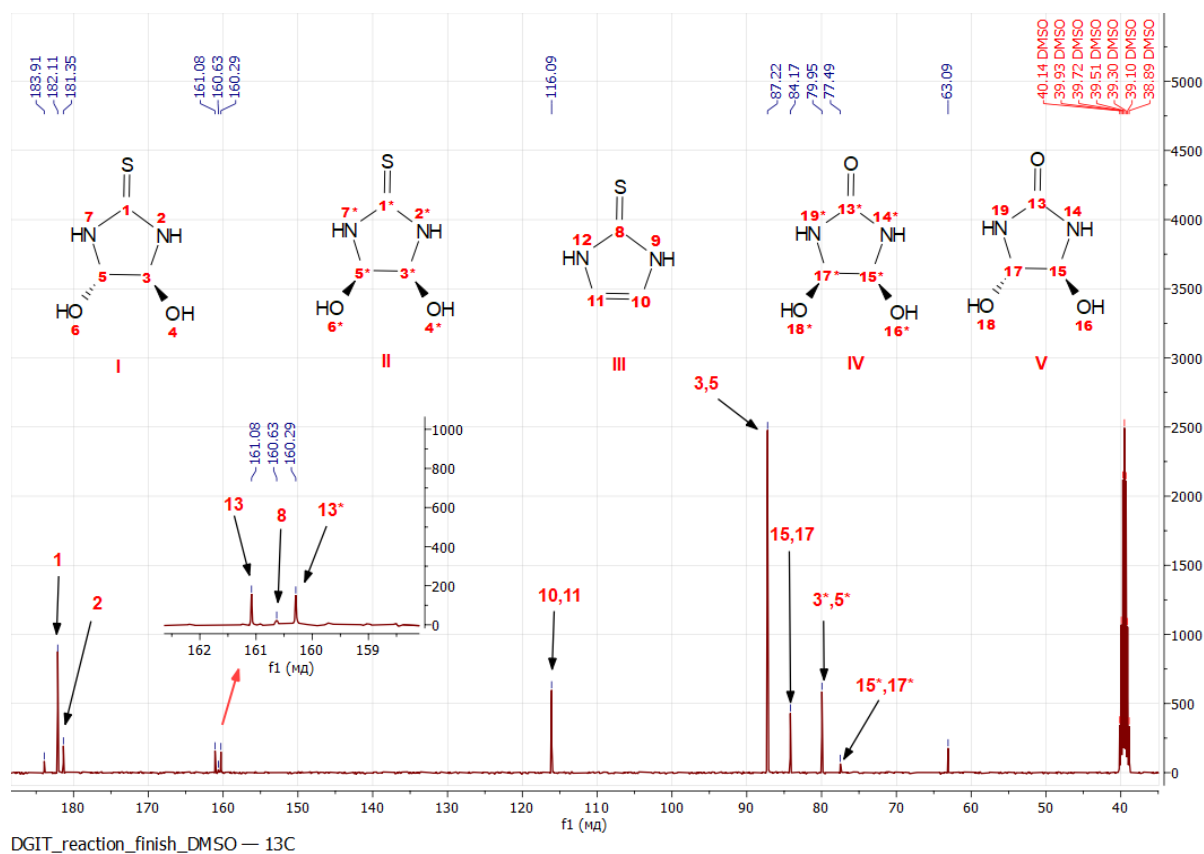


Figure 4. ^{13}C NMR spectrum of concentrated reaction mixture in $\text{DMSO}-d_6$

Table 1. Value of deuterium isotope shifts in ^{13}C NMR in $\text{H}_2\text{O}/\text{D}_2\text{O}$

^{13}C NMR chemical shifts, ppm	DIS, ppm	Fragment of molecule	^{13}C NMR chemical shift, ppm		DIS, ppm	Fragment of molecule
181.76 181.67	0.08	-C-HN-(D)	86.41	86.29	0.12	-C-HO-(D)
180.68 180.63	0.06	-C-HN-(D)	83.46	83.35	0.11	-C-HO-(D)
162.56 162.5	0.06	-C-HN-(D)	79.77	79.66	0.11	-C-HO-(D)
154.8 154.72	0.08	-C-HN-(D)	77.35	77.25	0.10	-C-HO-(D)
116.81 116.67	0.14	-C-HN-(D)	62.58	—	—	—

To understand the appearance of doublets, the ^{13}C NMR spectra of pristine DHIT (Aldrich, S169978) in $\text{DMSO}-d_6$, D_2O and $\text{H}_2\text{O}/\text{D}_2\text{O}$ were recorded. The doublets in the spectrum in $\text{H}_2\text{O}/\text{D}_2\text{O}$ were also observed. This can be due to the deuterium exchange of the protons of the amide and hydroxyl groups (Figure 5).¹⁴ The middle of the doublets shifts towards a high-field direction relative to singlet, which can be due to the replacement of the light hydrogen with heavier deuterium that leads to an increase in screening.

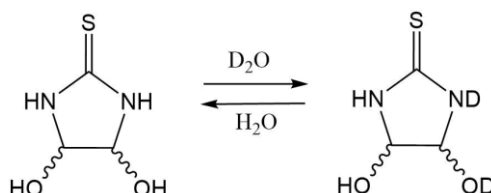


Figure 5. Scheme of hydrogen–deuterium exchange for DHIT in $\text{H}_2\text{O}/\text{D}_2\text{O}$

In the reference,¹⁵ the difference between the chemical shifts in the ^{13}C NMR spectrum in the presence of deuterium oxide compared to water is called a deuterium isotope shifts (DIS): $\text{DIS} = \delta(\text{H}_2\text{O}) - \delta(\text{D}_2\text{O})$. The value of DIS in the ^{13}C NMR depends on the neighboring groups that include protons capable of being replaced by deuterium, and does not depend on the temperature. Thus, this value allows determining which group is bound to carbon in this molecule. In the present work, the protons that can be replaced by deuterium are bonded with heteroatoms of oxygen ($-\text{OH}$) and nitrogen ($-\text{NH}-$). In the mixed solvent ($\text{H}_2\text{O}/\text{D}_2\text{O}$), the shape of lines of the $-\text{C}-\text{OH}(\text{D})$ and $-\text{C}-\text{NH}(\text{D})$ signals is highly dependent on the H/D exchange rate. Usually, amide $\text{C}-\text{NH}(\text{D})$ exchange is rather slow, and the signals appear as "singlet", however, the alcohol $-\text{C}-\text{OH}(\text{D})$ exchange is rather rapid, and the signals appear as "doublet". These are the temperature dependent events. However, the reaction mixture was diluted in cold D_2O , and NMR spectra were recorded. Thus, the NMR analysis of the sample was carried out at a temperature of about $10\text{ }^\circ\text{C}$, and the amide $\text{C}-\text{NH}(\text{D})$ and alcohol $-\text{C}-\text{OH}(\text{D})$ exchanges were observed. This means that the DIS value for the quaternary carbon atoms identified above, (for *trans*- and *cis*-DHIT these are 0.08 and 0.06 ppm that can be assigned to the fragment $=\text{C}-(\text{NH}(\text{D}))_2-$). The same fragment with the same DIS should correspond to the signals at 162.5 ppm and 154.8 ppm. Its signals are shifted upfield (that is, a lower chemical shift) in comparison with the thioamide group of the DHIT presumably indicating the replacement of sulfur with more electronegative oxygen.¹⁶

Thus, by analogy with the carbon of the methine groups of *cis*-, *trans*-DHIT with the DIS values of 0.12 ppm and 0.11 ppm, respectively, the signals in the range of 86.25–77.25 ppm corresponds to the fragment $-\text{C}-\text{OH}(\text{D})$. The only signal is 62.58 ppm in ^{13}C NMR spectrum as a singlet, since the hydrogen–deuterium

exchange does not occur or its speed is high, and its effect is not observed when the spectrum is taken under standard conditions. In this region of the spectrum, the signals correspond to $-\text{CH}_3$ or $-\text{CH}_2$ groups.

Using the DEPT 135 of the reaction mixture in $\text{DMSO}-d_6$ that allows isolating various types of substitution of carbon atoms, it was confirmed that the signals in the range from 183 to 160 ppm and 116 ppm can be assigned to the quaternary carbon atoms, and those directed in one direction with methine carbon atoms in DHIT (87.22, 84.17, 79.95, 77.49) are assigned to the $-\text{CH}$ groups, while the one directed downwards (63.09 ppm) is related to $-\text{CH}_2$ group that confirms our assumption above.

The 2D $^{13}\text{C}-^1\text{H}$ HSQC and $^{13}\text{C}-^1\text{H}$ HMBC spectra were recorded to determine the correspondence between the H - C atoms. The $^{13}\text{C}-^1\text{H}$ HSQC spectrum shows direct correlations between the C - H atoms, and the $^{13}\text{C}-^1\text{H}$ HMBC spectrum that characterizes the long-range correlation of the carbon atoms with protons allows the sequencing of carbon atoms in the molecule to be established (Table 2). The signals of the methine groups in *cis*-DHIT with direct $^{13}\text{C}-^1\text{H}$ (79.95 ppm - 5.04 ppm) and long-range (8.67-79.9 ppm) correlations as well as *trans*-DHIT with direct (87.2 ppm - 5.5 ppm) and two long-range correlations (6.29 ppm, 87.21 ppm; 8.8 ppm 188 ppm) were identified.

Based on DIS (Table 1), the carbon of the methyl group (84.17 ppm) with a direct $^{13}\text{C}-^1\text{H}$ correlation (84.17 ppm - 4.58 ppm) is bonded to the $-\text{OH}$ group. The long-range correlation of the carbon atom of the same group with a proton at 7.12 ppm can be assigned to $-\text{NH}$ group (Table 2). These results indicate that the signals related to protons of the amino and methine groups as well as the carbon of the methine group are shifted upfield. In comparison with the signals of the *trans*-DHIT, this occurs due to their shielding by a more electronegative element than sulfur, e.g., oxygen of the amide group, which is located in the region of 160 ppm.

The ratio of methine and amino groups signals intensity NH:CH are 1.53:1.53. This suggests that the signal in the ^1H NMR spectrum in the form of doublet at 5.9 ppm with the integral intensity of 1.53, is related to a hydroxyl group. Thus, the presumably identified compound is 4,5-dihydroxyimidazolidin-2-one. There are three signals in this area and two of them have no correlation, those at 161.08 ppm and 160.29 ppm in Figure 4.

To select the amide signal, we consider similar carbon of the methine group (77.49 ppm), which is also bonded with the $-\text{OH}$ group (Table 2) and has a direct correlation with the proton at 4.92 ppm. A slight shift of the methine group into the region of the strong field, protons of the amino and hydroxyl groups as well as the ratio of integral intensities NH:CH:OH (0.83: 0.85: 0.85) suggest that the compound with the signals in the high field is *cis*-4,5-dihydroxyimidazolidin-2-one (*cis*-DHI, compound IV in Figures 3, 4), in a weaker field - *trans*-4,5-dihydroxyimidazolidin-2-one (*trans*-DHI, compound V in Figures 3, 4). Thus, the signal at 160.29 ppm is the amide group of *cis*-DHI and the signal at 161.08 ppm is related to *trans*-DHI. The identified signals are consistent with the literature data.¹⁷

The last unidentified quaternary carbon atom signal at 160.63 ppm has a ^{13}C - ^1H long-range correlation with the proton at 6.81 ppm, which has a direct correlation with the methine group at 116.09 ppm (Table 2). The proton of the methine group in this region of the spectrum belongs to the compounds with a double bond. The magnetic anisotropic effect of the double bond leads to the deshielding of the methine group at 116.09 ppm and its downfield shift compared to the *trans*-DHIT also to the screening of the protons of the NH group and the shift to the high field with a value of 11.91 ppm and the thioamide group at 160.63 ppm (Figures 3, 4). According to the integral intensities, the NH:CH ratio is 2:2, that is, the number of amino and methine protons is the same, therefore, the identified substance is 1,3-dihydro-2*H*-imidazole-2-thione (compound III in Figures 3, 4).¹⁸ The structure III shows that the carbon atoms 11 and 12 (Figure 4) interact with the protons 9, 12. This fact does not contradict with the assumptions in Table 1.

In dynamic NMR analysis in DMSO-*d*₆, the signal intensity at 63.09 ppm related to methyl group with a direct proton correlation with 3.38 ppm does not change; therefore, we assume that this is the signal of the methyl group of glycolic acid, which was an impurity in glyoxal. The unidentified signal at 183.91 ppm (Figure 4) can be assigned to the carbonyl group of this acid.¹⁹ The absence of the deuterium exchange in the ^{13}C NMR spectrum in the H₂O/D₂O solvent also confirms the assumption, because the deuterium exchange in carboxylic acids occurs at high rate and is difficult to detect when recording the spectrum under these conditions.

Table 2. Results of 2D ^{13}C - ^1H HSQC and ^{13}C - ^1H HMBC experiments

Direct correlation of ^1H - ^{13}C NMR		Multiplicity	Fragments of molecule	Long-range correlation of ^1H - ^{13}C NMR		Fragments of molecule
^{13}C	^1H			^1H	^{13}C	
63.09	3.38	s	—CH ₂	—	—	—
77.49	4.92	d	—CH (<i>cis</i> -DHI)	—	—	—
79.95	5.04	d	—CH (<i>cis</i> -DHIT)	8.67	79.95	-CH-CH-NH-
84.17	4.58	d	—CH (<i>trans</i> -DHI)	7.12	84.17	-CH-CH-NH-
87.22	4.71	d	—CH (<i>trans</i> -DHIT)	6.29	87.21	-CH-OH
				8.86	182.11	-CH-CH-NH-
116,09	6.81	s	—C=C—	6.81	160,63	-CH-CH-NH-

Thus, using NMR spectroscopy it was found that the byproducts formed during the DHIT preparation are 1,3-dihydro-2*H*-imidazole-2-thione (III), *cis*-DHI (IV), and *trans*-DHI (V) (Figures 3, 4). Table 3 shows all NMR results.

Table 3. Results of reaction mixture analysis by NMR in DMSO-*d*₆

¹ H NMR chemical shifts, ppm			¹³ C NMR chemical shifts, ppm			Substance	Literature
-NH-	-CH-	-OH	-C=O	-C=S	-CH-		
8.67	5.03	5.84	-	181.35	79.95	<i>cis</i> -DHIT	13
8.86	4.73	6.04	-	182.11	87.22	<i>trans</i> -DHIT	13
11.91	6.81	-	-	160.09	116.09	1,3-dihydro-2 <i>H</i> -imidazole-2-thione	18
6.95	4.91	5.5	-	161.08	77.49	<i>cis</i> -DHI	17
7.12	4.59	5.85	160.29	-	84.17	<i>trans</i> -DHI	17

In dynamic NMR analysis, after the formation of compounds I and II, there is an increase in the intensity of the signal of protons 10, 11 of compound III, then the signals 17, 15 of compound V and the signals 17*, 15* of compound IV (Figure 3), which indicates the sequence of formation of compounds. The presence of oxygen-containing analogues of DHIT (V, IV) indicates the glyoxal interaction with urea, but initially urea was absent in the reaction mixture, most likely it is formed as a result of the reaction. According to our assumption, by analogy with the mechanism of thiourea interaction with benzil,¹⁰ thiourea interacts with protonated DHIT to form urea and compound III, then urea interacts with glyoxal to form DHI (Figure 6).

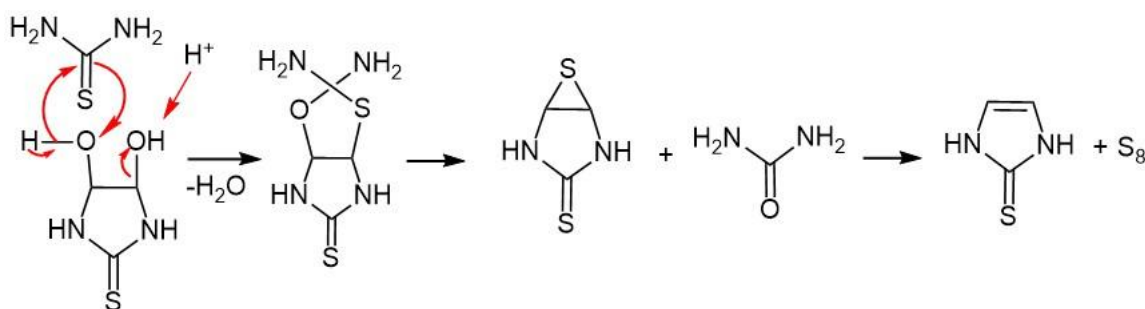


Figure 6. Scheme of formation of the urea and the 1,3-dihydro-2*H*-imidazole-2-thione (III)

Kinetic model

Figure 7 shows a diagram of the DHIT formation and side reactions occurring in the reacting system:

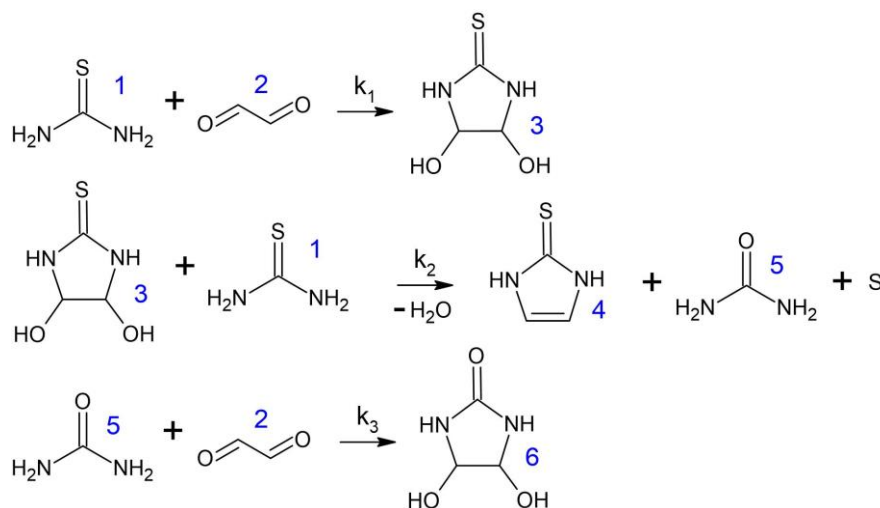


Figure 7. Reactions pathway

The reaction scheme is described by the ordinary differential equations (ODE) system containing 3 kinetic constants (Figure 7). Kinetic parameters k_1 , k_2 , k_3 were found as coordinates of the minimum of the sum of squares of deviations of the calculated concentrations of thiourea and DHIT according to the model from the experimental data. The minimum was searched using the Nelder-Mead algorithm with multiple starts.²⁰ To find the calculated concentrations, the ODE system (Figure 8) was numerically integrated using a semi-implicit two-stage L-stable Rosenbrock scheme with complex coefficients (4 orders of precision).²¹

$$\begin{aligned}
 c_1' &= -k_1 c_1 c_2 - k_2 c_1 c_3 \\
 c_2' &= -k_1 c_1 c_2 - k_3 c_5 c_2 \\
 c_3' &= k_1 c_1 c_2 - k_2 c_3 c_1 \\
 c_4' &= k_2 c_3 c_1 \\
 c_5' &= k_2 c_3 c_1 - k_3 c_5 c_2 \\
 c_6' &= k_3 c_5 c_2 \\
 c_1(0) &= c_1^0, c_2(0) = c_2^0, c_3(0) = c_4(0) = c_5(0) = c_6(0) = 0
 \end{aligned}$$

Figure 8. Kinetic model: c_i is a concentration of the i -th substances from the scheme in Figure 7 (mol/L),

k_i is a rate constant $(\text{mol/L})^{-1} \cdot \text{s}^{-1}$

The calculation was carried out based on a series of condensing grids with an estimate of the calculation error by the Richardson method.²²

The calculated values of the kinetic parameters are: $k_1 = 7.75 \cdot 10^{-1} (\text{mol/L})^{-1} \cdot \text{s}^{-1}$, $k_2 = 2.21 \cdot 10^{-2} (\text{mol/L})^{-1} \cdot \text{s}^{-1}$, $k_3 = 3.53 \cdot 10^{-7} (\text{mol/L})^{-1} \cdot \text{s}^{-1}$. Figure 9 shows a comparison of the calculated curve according to the model with the experimental data. It can be seen that the proposed scheme is consistent with the experimental data.

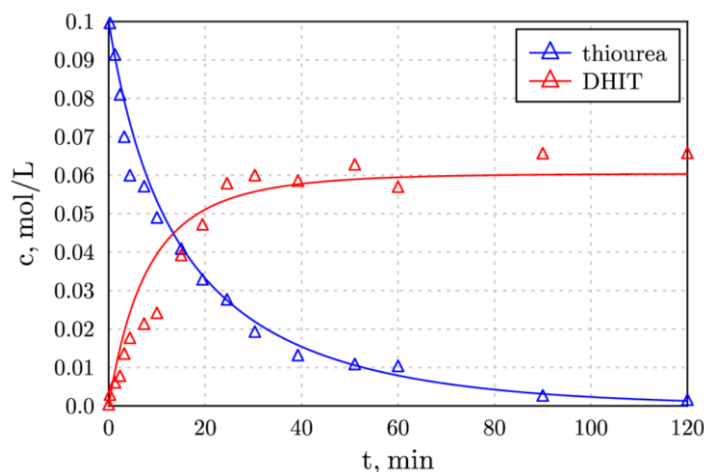


Figure 9. Kinetic curves of DHIT synthesis: triangles - experimental data, line - model calculation with found coefficients

The adequacy of the proposed scheme can be confirmed by the ability of the mathematical model built on the basis of the scheme to adequately describe the experimental data.

CONCLUSIONS

In this study we used HPLC method to determine thiourea and DHIT concentrations, and the kinetic curves were obtained.

Using NMR (DEPT135, ^{13}C - ^1H HSQC, ^{13}C - ^1H HMBC) the target products such as *cis*-, *trans*-isomers of DHIT and byproducts such as 1,3-dihydro-2*H*-imidazole-2-thione and *cis*-, *trans*-4,5-dihydroxyimidazolidin-2-one were identified for the thiourea reaction with glyoxal. Deuterium exchange of amido and hydroxyl protons of the target and byproducts in the mixed solvent (in $\text{H}_2\text{O}/\text{D}_2\text{O}$) was discovered. The DIS values allowed identifying the carbon signals in the ^{13}C NMR spectra.

The scheme of reactions explaining their formation was proposed: DHIT reacts with thiourea to form 1,3-dihydro-2*H*-imidazole-2-thione and urea, which, in turn, interacts with glyoxal to form 4,5-dihydroxyimidazolidin-2-one.

The kinetics of the scaled synthesis process was investigated, and the kinetic parameters of the model based on the proposed reaction scheme were calculated. The model described well the kinetics of the DHIT formation and thiourea consumption. The model can be used in process modeling and simulation of the reaction equipment.

EXPERIMENTAL

HPLC. HPLC analysis was performed on the HPLC Agilent 1200 equipped with an autosampler with built-in thermostat column compartment G1316A, a four-channel gradient pump G1311A and the DAD G1315D

detector. The column Luna HILIC 200 A 4.6 × 150 mm, 5 μm particle size (Phenomenex, USA) was used; column temperature was 30 °C; flow rate was 1.5 mL/min; injection volume was 5 μL. Detection was carried out at a wavelength of 245 nm; mobile phase was acetonitrile (MeCN):Water 97v/3v.

Kinetic experiment. The kinetics experiment was carried out in a 1L glass reactor with an overhead stirrer (Atlas, Manufacturer: Syrris, UK) equipped with a temperature control LT-300-N Laboratory electronic thermometer and a pH measurement by pH meter/ionomer ITAN.

A solution of thiourea and glyoxal in purified water was mixed at a temperature of 30 °C. The 1M solutions were used. A 2 mL aliquot of the reaction mixture was placed in a pre-suspended vial with 0.6 mL MeCN at 2-5 °C to stop the reaction, then HPLC analysis was carried out. Then the vials were weighed and the concentrations of thiourea and DHIT were determined based on the area of the chromatographic peak taking into account the dilution with MeCN. The samples were stored in the refrigerator at 2-5 °C prior to the analysis. The first 20 min of reaction were tested every 2 min followed by a 5–10-min interval.

NMR. NMR spectra were recorded on the Bruker Avance III HD spectrometer (Bruker BioSpin GmbH, Germany) operating at 400 MHz. The reaction mixture was taken from the 400 μL reactor to an NMR vial, 200 μL cold D₂O was added, and spectra were recorded. At the end of the reaction, the mixture was concentrated at 30 °C and a residual pressure, then NMR spectra were recorded in DMSO-*d*₆.

Materials. The MeCN for HPLC experiments was purchased from PanReac AppliChem (Castellar del Valles, Barcelona). Water was purified using a Milli-Q purification system (Merck Millipore, USA). Solvents for NMR experiments: DMSO-*d*₆ with 99.8 atom % D, D₂O with 99.8 atom % D were purchased from Solvex Co. Ltd. (Moscow, Russia). 40 wt.% aqueous glyoxal solution containing less than 1% of organic acids and thiourea (99+%) were all purchased from Acros Organics (Fair Lawn, NJ, USA).

REFERENCES

1. Yu. V. Nelyubina, G. A. Gazieva, V. V. Baranov, P. A. Belyakov, A. O. Chizhov, K. A. Lyssenko, and A. N. Kravchenko, *Russ. Chem. Bull., Int. Ed.*, 2009, **58**, 1353.
2. V. V. Baranov, A. A. Galochkin, Y. V. Nelyubina, A. N. Kravchenko, and N. N. Makhova, *Synthesis*, 2020, **52**, 2563.
3. M. Singh, E. Solel, E. Keinan, and O. Reany, *Chem. Eur. J.*, 2014, **21**, 536.
4. C. Lang, A. Mohite, X. Deng, F. Yang, Z. Dong, J. Xu, J. Liu, E. Keinan, and O. Reany, *Chem. Commun.*, 2017, **53**, 7557.
5. F. N. Tehrani, K. I. Assaf, R. Hein, C. M. E. Jensen, T. C. Nugent, and W. M. Nau, *ACS Catal.*, 2022, **12**, 2261.
6. T. S. Lobana, Sultana R., G. Hundala, and R. J. Butcher, *Dalton Trans.*, 2019, **48**, 4124.
7. A. Nikulina, L. Kalichkina, and V. Malkov, Patent 2017, RU 2625312 C1.

8. M. Singh, G. Parvari, M. Botoshansky, E. Keinan, and O. Reany, [*J. Org. Chem.*, 2014, **5**, 933.](#)
9. Q. Long, G. Hong, H. Ding, and Y. Hauxue, *Chinese J. Org. Chem.*, 1982, **3**, 170.
10. C. J. Broan and A. R. Butler, [*J. Chem. Soc., Perkin Trans. 2*, 1991, 1501.](#)
11. V. P. Tuguldurova, O. A. Kotelnikov, R. S. Cheltygmasheva, A. A. Bakibaev, and O. V. Vodyankina, [*J. Struct. Chem.*, 2020, **61**, 225.](#)
12. V. P. Tuguldurova, A. V. Fateev, V. S. Malkov, O. K. Poleshchuk, and O. V. Vodyankina, [*J. Phys. Chem. A*, 2017, **121**, 3136.](#)
13. K. Mamko, L. Kalichkina, O. Kotelnikov, A. Nikulina, N. Dementeva, and D. Novikov, [*Chromatographia*, 2020, **83**, 1087.](#)
14. S. Hanashima, K. Katobc, and Y. Yamaguchi, [*Chem. Commun.*, 2011, **47**, 10800.](#)
15. S. Tassoti, M. Walenta, A. Pöcheim, K. Buchberger, O. Kunert, and K. Zangger, *Analyst*, 2019, **144**, 7463.
16. T. Fiala, K. Sleziakova, K. Marsalek, K. Salvadori, and V. Sindelar, [*J. Org. Chem.*, 2018, **83**, 1903.](#)
17. H. D. Correia, R. S. Cicolani, R. F. Moral, and G. J. F. Demets, *Synthesis*, 2016, **48**, 210.
18. B. V. Trzhtsinskaya and N. D. Abramova, [*Sulfur Reports*, 1991, **10**, 389.](#)
19. C. Dai, L. Sun, H. Liao, B. Khezri, R. D. Webster, A. C. Fisher, and Z. J. Xu, [*J. Catal.*, 2017, **356**, 14.](#)
20. J. A. Nelder and R. Mead, [*Comput. J.*, 1965, **7**, 308.](#)
21. A. B. Alshin and E. A. Alshina, [*Math. Models Comput. Simul.*, 2011, **3**, 604.](#)
22. E. A. Alshina, N. N. Kalitkin, and P. V. Koryakin, *Comput. Math. Math. Phys.*, 2005, **45**, 1769.